



Thermophysical Model of (269) Justitia—Main Belt Asteroid Possibly Implanted from Trans-Neptunian Region

Anna Marciniak¹, Antoine Choukroun¹, Julia Perla¹, Waldemar Ogłóża², Robert Szakáts^{3,4}, Pierre Antonini⁵, Raoul Behrend⁵, Géza Csörnyei⁶, Marek Drózdź², Marcel Fauvaud^{7,8}, Stéphane Fauvaud^{7,8}, Adrian Jones⁹, Dong-Heun Kim¹⁰, Myung-Jin Kim¹¹, Viktor Kudak¹², Iga Mieczkowska¹, Erika Pakštienė¹³, Vasyl Perig¹², and Eda Sonbas^{14,15}

¹ Astronomical Observatory Institute, Faculty of Physics and Astronomy, Adam Mickiewicz University, Stoleczna 36, 60-286 Poznań, Poland

² Mount Suhora Observatory, University of the National Education Commission, Podchorążych 2, 30-084, Cracow, Poland

³ Konkoly Observatory, HUN-REN Research Centre for Astronomy and Earth Sciences, Konkoly Thege 15-17, H-1121 Budapest, Hungary

⁴ CSFK, MTA Centre of Excellence, Budapest, Konkoly Thege Miklós út 15-17, H-1121, Hungary

⁵ Geneva Observatory, CH-1290 Sauverny, Switzerland

⁶ Konkoly Observatory, Research Centre for Astronomy and Earth Sciences, Eötvös Loránd Research Network (ELKH), H-1121 Budapest, Konkoly Thege Miklós út 15-17, Hungary

⁷ Observatoire du Bois de Bardou, 16110 Taponnat, France

⁸ Association T60, Observatoire Midi-Pyrénées, 14, avenue Edouard Belin, 31400 Toulouse, France

⁹ British Astronomical Association, Burlington House, Piccadilly, Mayfair, W1J 0DU, London, UK

¹⁰ Chungbuk National University, 1, Chungdae-ro, Seowon-gu, Cheongju-si, Chungcheongbuk-do, Republic of Korea

¹¹ Korea Astronomy and Space Science Institute, 776 Daedeok-daero, Yuseong-gu, Daejeon 34055, Republic of Korea

¹² Laboratory of Space Researches, Uzhhorod National University, Daleka st. 2a, 88000, Uzhhorod, Ukraine

¹³ Institute of Theoretical Physics and Astronomy, Vilnius University, Saulėtekio al. 3, 10257 Vilnius, Lithuania

¹⁴ Department of Physics, Adiyaman University, Adiyaman 02040, Türkiye

¹⁵ Astrophysics Application and Research Center, Adiyaman University, Adiyaman 02040, Türkiye

Received 2024 June 20; revised 2024 September 24; accepted 2024 October 16; published 2025 March 18

Abstract

Asteroid Justitia is a special main-belt object, being an extremely red body with a steeper spectral slope than any other D-type asteroid. Conversely, its spectral and polarimetric properties resemble organics-rich Centaurs and trans-Neptunian objects. For this reason, it was chosen as a main target of the MBR Explorer space mission. It is crucial for space mission planning and operations to have in advance the best estimate of the target size, spin, shape, and properties of the surface. In particular, the size determination was in high demand before the extensive stellar occultation campaign in 2023 August, for station deployment and observation planning. We utilized multiple lightcurves from our campaign on slow rotators and from the literature to reconstruct the spin and shape of Justitia via lightcurve inversion. Then we applied the Convex Inversion Thermophysical Model to simultaneously optimize the fit to visible lightcurves and to thermal data from infrared space observatories. We present here the pair of most precise physical models of Justitia possible before the occultation campaign, with similar properties of both solutions. The size range of Justitia was narrowed here to 55–60 km, so by a factor of 4 compared with previous estimates, and also the shape model's resolution was improved. An estimate of thermal inertia and surface roughness was also obtained, with implications for surface texture and regolith properties.

Unified Astronomy Thesaurus concepts: Asteroids (72); Asteroid surfaces (2209); Asteroid rotation (2211)

Materials only available in the [online version of record](#): data behind figure, figure set

1. Introduction

Asteroid (269) Justitia studied by spectroscopy revealed unusual features. In the research of F. E. DeMeo et al. (2009) and S. Hasegawa et al. (2021), this D-type asteroid was found to have an extremely red surface color and a much steeper spectral slope than any other D-type asteroid (the red spectrum meaning increased reflectance toward longer wavelengths). The recent classification scheme of asteroid spectra by M. Mahlke et al. (2022) actually separates the extreme, red-sloped objects into a new “Z-class”. Justitia, and (203) Pompeja, distinctively stand out of their taxonomy, looking clearly out of place. Their spectra are much more typical for the outer solar system trans-Neptunian and Centaur objects of RR and IR class, rich in organics (S. Hasegawa et al. 2021). To create a surface with

such an extremely red spectrum requires a presence of complex organic matter. For such matter to be created, ices of volatile organic matter are necessary, like methanol and methane (C. Sagan & B. N. Khare 1979), although the signatures of such (fresh) ices are today absent from their surface spectra due to organic ice reddening. This implies that objects bearing such compounds must have formed beyond the snow line of certain volatile organics, while objects with bluer surface spectra (BB and BR type) formed inside of this line (P. Vernazza & P. Beck 2017).

Moreover, asteroid (269) Justitia has been found to display quite unusual polarimetric properties (R. Gil-Hutton & E. García-Migani 2017). Similarly to a Centaur Chariklo and the dark side of Saturn's moon Iapetus, it has the smallest depth of negative polarization branch of all bodies ever subjected to polarimetric studies, and also a very small angle of minimum polarization. Such properties put it close to dark F-type asteroids and icy objects, yet far from D-type Jupiter Trojans.

All these findings strongly suggest that asteroid Justitia has been formed in the outer solar system and later was transported



Original content from this work may be used under the terms of the [Creative Commons Attribution 4.0 licence](#). Any further distribution of this work must maintain attribution to the author(s) and the title of the work, journal citation and DOI.

to the main belt during the planetary migration era (A. Morbidelli et al. 2005; K. Tsiganis et al. 2005; D. Vokrouhlický et al. 2016). The fact that objects of such properties are so rare in the inner solar system would be a simple consequence of their origin in the farther regions of the outer solar system, as compared to, e.g., D-type Jupiter Trojan asteroids, believed to evolve from BR-type trans-Neptunian objects (S. Hasegawa et al. 2021).

As such, this object provides a unique opportunity to study outer solar system objects in situ without a lengthy space mission. Its relatively good accessibility (middle main belt), together with unique features, providing constraints on solar system formation and dynamic evolution, were the main drivers of the recently announced Mohammed bin Rashid (MBR) Explorer space mission (G. Filacchione et al. 2023; A. Raponi et al. 2023) of the United Arab Emirates (UAE),¹⁶ also known as the Emirates Mission to the Asteroid Belt. The mission launch is scheduled for 2028 March. The spacecraft is planned to visit seven asteroids and attempt to land on Justitia in the year 2034. This mission is well in line with the white paper advocating the need for a space mission to a primitive main-belt asteroid (P. Vernazza et al. 2022).

The science objectives of the MBR Explorer mission are, among others, to provide new insights into the dynamical evolution of small main-belt asteroids and to help investigate how icy small bodies physically evolve across the solar system. One of the principal goals of the mission is to determine the geological history, interior structure, and ice content of the target asteroids (M. R. El-Maary et al. 2023). These general science goals are going to be achieved with the four instrument main payload: a visible narrow-angle framing camera, a midwavelength infrared (IR) imaging spectrometer, an IR spectrometer, and an IR imager (H. Reed et al. 2023). Using these instruments, the mission in particular is going to determine the asteroids' mineralogy, including hydrated minerals, and their organic materials content; derive the surface regolith properties; characterize the diurnal surface temperature and its temporal variability; determine the thermophysical properties of the outer surface layers; and characterize the potential landing zones on (269) Justitia (G. Filacchione et al. 2023).

Since the announcement of the mission, the scientific interest in Justitia has started to grow. For example, a promising stellar occultation by Justitia has been predicted for 2023 August 31, and an extensive campaign has been organized, with over 50 observers engaged (see M. W. Buie et al. 2025).

By a fortunate coincidence, we had been observing Justitia within our photometric campaign targeted at slow rotators (A. Marciniak et al. 2015) for a few years already when the mission to this asteroid was announced. During this campaign, we have been gathering dense rotational lightcurves of a few tens of asteroids with periods within a range of 12–60 hr, to construct their spin and shape models and put them into scale via thermophysical modeling and stellar occultations (see, e.g., A. Marciniak et al. 2021, 2023). At the request of the occultation team gathered around the event in 2023 August, we attempted to determine the size of Justitia, to help with the planning of the station deployment. Previous size determinations of this asteroid ranged from 46.56 ± 1.655 km (E. L. Ryan & C. E. Woodward 2010) to 64.92 ± 0.590 km (J. R. Masiero et al. 2012), with the newest determination of

60.94 ± 13.950 (J. R. Masiero et al. 2020), complicating the occultation campaign planning that aimed at dense and uniform coverage of the predicted asteroid shadow.

Combining lightcurves from our slow rotators program with the data from the literature, we successfully reconstructed Justitia's spin and shape, first basing this exclusively on relative lightcurves. Later we combined these lightcurves with thermal data in a joint approach that resulted in a comprehensive model of the spin, shape, size, and thermal inertia of Justitia. This model provided the size in a much narrower range than published before, allowing for an optimal station deployment plan and contributing to the success of the occultation campaign (M. W. Buie et al. 2025).

In the following section, we briefly describe previous photometric studies on Justitia and our program targeting slow rotators. The next section outlines the methods used for spin and shape reconstruction, followed by the thermophysical modeling description and the results. Section 4 summarizes the work and outlines prospects for the utilization of our results.

2. Photometric Observations

Long before Justitia was chosen as a target of a space mission, it was part of our program targeting slow rotators. These are asteroids whose spin and shape models were often unavailable, due to observing selection effects. Their long rotation periods, in the range of 12–60 hr, often coupled with small amplitudes of lightcurves, make them challenging targets largely avoided by previous studies (A. Marciniak et al. 2015). Due to the scarcity of dense lightcurves, construction of their spin and shape models was hampered, and as a consequence this bias made them underrepresented in the sample of well-studied asteroids, considering their actual, abundant occurrence (see, e.g., A. Pál et al. 2020).

Our photometric observing campaign targeted at slow rotators is described in detail in A. Marciniak et al. (2015). In the case of Justitia, stations from Turkey, Lithuania, Hungary, Poland, Ukraine, the UK, France, and South Korea provided data that resulted in almost full coverage of Justitia's 33 hr period in all three attempted apparitions. Telescopes with diameters from 30 to 60 cm equipped with CCD cameras were used, and the observations were made mostly through R but also L filters. They were long (3–9 hr), continuous exposure series of the field with the asteroid and comparison stars, resulting in precise, dense lightcurves. The key issue in the campaign targeting slow rotators is the observers' coordination for efficient phase coverage and duplicate avoidance. It was achieved with an internal web planning service displaying visible targets, their rotation phases already covered, and those available during a given night from a particular observing site. Some duplication of lightcurve fragments was actually desirable, especially spaced by a few weeks, since the repeating lightcurve features facilitate better constraining the rotation period, but also track the small lightcurve morphology changes due to shadowing effects. The raw CCD frames have been corrected for bias, dark frame, and flat field, and the aperture photometry was applied using various software. When, due to asteroid brightness, short exposures have been used, to avoid oversampling a point binning was applied so that the number of data points per period stayed between 100 and 200.

Figures 5–6 present the composite lightcurves from three apparitions obtained within this study. Table 2 presents the observing runs' circumstances, the observers, and their sites.

¹⁶ MBR Explorer was named after Sheikh Mohammed bin Rashid Al Maktoum, the vice president and prime minister of UAE.

Previously, lightcurves of Justitia have been published by M. A. Barucci et al. (1992), F. Pilcher (2016), and T.-S. Yeh et al. (2020). The rotation period of 16.5 hr from the first and last of these works was found to be twice as long by F. Pilcher (2016), which has been confirmed by our observations.

3. Modeling Asteroid Justitia

By another lucky coincidence, in mid-2023 the overall set of Justitia lightcurves from our program and the literature turned out to be just sufficient for spin and shape reconstruction. Also, there existed a rich set of thermal data from infrared observatories. All this combined allowed us to determine the size of this body just in time for the occultation campaign on 2023 August 31.

First, we used exclusively the relative lightcurves in the visible for an initial spin and shape reconstruction through the lightcurve inversion method (M. Kaasalainen & J. Torppa 2001; M. Kaasalainen et al. 2001). The shape model in this method is a convex polyhedron parameterized by a spherical harmonics series. When the method is fed with data from sufficiently varied viewing geometries, it quickly converges to a unique solution. We constrained both the period and the spin solution for Justitia this way, with its pole mirror counterpart, due to the unavoidable symmetry of the problem. Since the majority of main-belt asteroids have low orbital inclinations, the appearance of their lightcurves would be insensitive to a mirror-flip of the spin axis by 180° in longitude. This ambiguity can only be broken for asteroids with orbital inclination higher than $\sim 20^\circ$. In the case of Justitia, its orbit inclination to the ecliptic I is 5.5° , so the spin and shape ambiguity is inevitable.

The lightcurves are well fitted by the models practically down to the noise level (0.010 mag; see Figure 7 in the Appendix). There existed a previous spin and shape model of Justitia, based exclusively on sparse-in-time data (J. Āurech et al. 2020). Our spin solutions are similar to it, but due to the usage of dense lightcurves, our initial shape model is less angular. However, the stretch of this initial model along the “z”-axis is not well constrained from the lightcurve inversion alone.

In the next step, we added one of two sparse photometric data sets from the ATLAS survey (J. L. Tonry et al. 2018), used by J. Āurech et al. (2020). These calibrated data well constrained the stretch of the shape model along the rotation axis, since they are sensitive to the absolute dimensions of the asteroid cross section. Then we gathered all available thermal data for Justitia, downloading them from the Infrared Database¹⁷ (R. Szakats et al. 2020). They were obtained at 12, 25, and 60 μm (IRAS survey; G. Neugebauer et al. 1984); 9 and 18 μm (Akari survey; F. Usui et al. 2011), and 22.6 μm (Wide-field Infrared Survey Explorer (WISE) survey; E. L. Wright et al. 2010). Data obtained by WISE at 11.1 μm were partially saturated and could not be used.

We utilized these data in a joint approach to optimize the asteroid parameters and shape simultaneously to fit the visible lightcurves, sparse data, and thermal flux measurements. This method is called the Convex Inversion Thermophysical Model (CITPM) and has been introduced by J. Āurech et al. (2017) and verified on multiple targets by A. Marciniak et al. (2021). In parallel to the same convex inversion algorithms

described above, the CITPM method also uses the standard Thermophysical Model (TPM) approach introduced by J. S. V. Lagerros (1996, 1997, 1998) and widely used in multiple thermophysical studies (see M. Delbo’ et al. 2015 for the review). The algorithm solves the one-dimensional heat diffusion equation to find the temperature of each surface element and its infrared flux at the time of each thermal measurement. There are hundreds of such surface elements, whose contribution is added for the overall flux. The parameters characterizing each element are thermal inertia, surface roughness (described by spherical-section craters of opening angle from 10° to 90° and fraction of surface coverage from 0% to 100%), and a light scattering law in the form of the Hapke model (B. Hapke 1981, 1984, 1986). Parameters of the Hapke model are optimized to fit the phase curve. For emissivity, we used a standard value of 0.9 (see, e.g., L. F. Lim et al. 2005). The main point in the CITPM usage is to find the best weight between visible and thermal data so that the final model optimally fits both types of data. Still, making the initial, convex inversion model based on lightcurves only was a necessary step. The CITPM method, due to the multitude of fitted parameters, is not able to scan the whole parameter space for the best period and spin axis position. Thus, the spin parameters from the convex inversion are a required input for the CITPM.

4. Results

Applying the CITPM we obtained a much smoother, more realistic shape model of Justitia than from lightcurve inversion alone, and a precise size determination with an estimate of thermal inertia and surface roughness. The resulting model parameters are presented in Table 1. The spin axis is far from the ecliptic plane and the rotation is retrograde, as indicated by the negative values of β_p . Size is now constrained to the narrow range of 55–60 km, where CITPM solutions even 2 km beyond this range provided a much poorer fit to thermal data. Shape models for both spin solutions are presented as viewed from three sides in Figure 1. In addition, Figure 2 shows the fit of both model solutions to a normalized phase curve, while Figures 7 and 8 show the model fit to lightcurves in the visible, and the fit to all the thermal data, respectively. It can be seen that this model well fits both types of data with very small deviations of model lightcurves from the observed ones (0.0128 mag) and a small reduced $\chi^2 = 0.29$ for the infrared data fit (all values discussed here are for pole 1 solution, those for the mirror solution being similar; see Table 1). Geometric albedo is also well constrained to 0.058 ± 0.006 .

Unlike the size and albedo, the thermal inertia is usually determined with a large uncertainty, and so is the case here: for pole 1 it is 41_{-40}^{+110} SI units, where most of the solutions with free thermal inertia tended to concentrate below 50 SI units. A large uncertainty here might be due to the relatively large variations in Justitia heliocentric distance (full range of the order of 0.6 au at the mean value of 2.74 au), while there is a dependence of thermal inertia on heliocentric distance, due to different temperatures (S. J. Keihm 1984; M. Mueller et al. 2010). Figure 4 present the results from multiple loops over various levels of surface roughness, run for thermal inertia varied by 10 SI units¹⁸ in each step. In Table 1 we also present the thermal inertia corrected to 1 au (87 SI units) for direct

¹⁷ <https://ird.konkoly.hu/>

¹⁸ $\text{J m}^{-2} \text{s}^{-1/2} \text{K}^{-1}$.

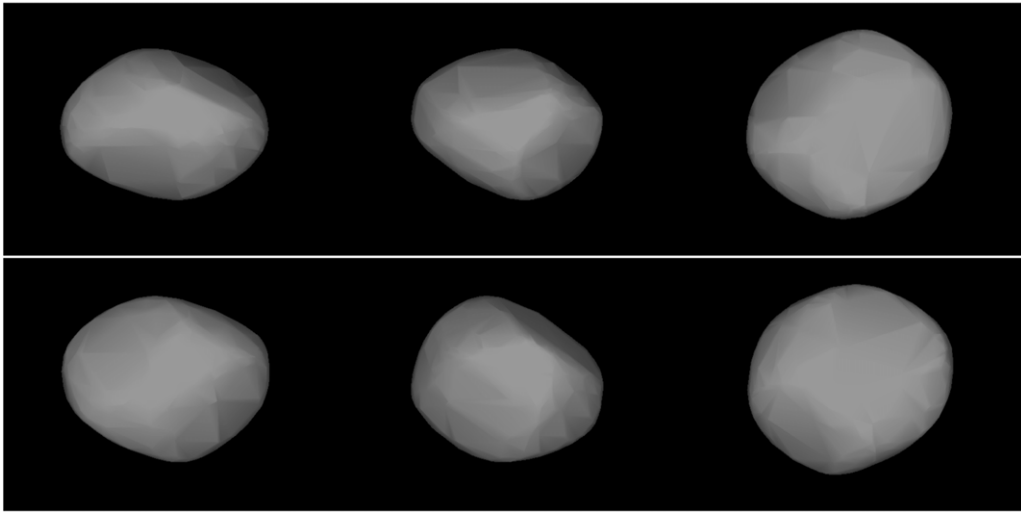


Figure 1. Shape models of asteroid (269) Justitia from the CITPM: solution for pole 1 (top) and pole 2 (bottom). Shapes are displayed in three views, left to right: two equatorial views, 90° apart, and a pole-on view.

Table 1

Physical Properties of Asteroid Justitia and Information on the Data Set Used

Parameter	Value
Number of apparitions (calendar years)	7 (1984–2022)
Number of lightcurves	52
Number of IRAS, Akari, and WISE thermal data points	12, 10, 15
Average heliocentric distance (au)	2.74 ± 0.30
Pole 1 solution	
λ_{p1} (deg)	73 ± 11
β_{p1} (deg)	-81 ± 15
Sidereal period (hr)	33.12962 ± 0.00001
Deviations from visible lightcurves (mag)	0.0128
Infrared χ^2_{red}	0.29
Equivalent sphere diameter (km)	58 ± 2
Albedo	0.058 ± 0.006
Thermal inertia (SIu)	41^{+110}_{-40}
Thermal inertia at 1 au (SIu)	87
Pole 2 solution	
λ_{p2} (deg)	254 ± 8
β_{p2} (deg)	-68 ± 12
Sidereal period (hr)	33.12962 ± 0.00001
Deviations from visible lightcurves (mag)	0.0124
Infrared χ^2_{red}	0.27
Equivalent sphere diameter (km)	56^{+4}_{-1}
Albedo	0.059 ± 0.007
Thermal inertia (SIu)	53^{+100}_{-52}
Thermal inertia at 1 au (SIu)	113

Note. The first two rows contain the number of apparitions when lightcurves were obtained, calendar years, and the number of separate lightcurves. The next part details the infrared data set: the number of points provided by space observatories IRAS, Akari, and WISE, respectively, and an average heliocentric distance of thermal infrared observations r_{hel} with the standard deviation. Next follow the model parameters for two mirror solutions: J2000 ecliptic coordinates λ_p , β_p of the spin axis, sidereal rotation period P , and the deviation of model fit from those lightcurves (including fit to sparse data). The next rows present the reduced chi-square of the best fit (χ^2_{red}) to infrared data, the surface-equivalent size D , geometric albedo p_V , thermal inertia Γ in $\text{J m}^{-2} \text{s}^{-1/2} \text{K}^{-1}$ SI units (SIu), and thermal inertia normalized to 1 au calculated according to the equation $\Gamma_{1 \text{ au}} = \Gamma(r)^{0.75}$, following B. Rozitis et al. (2018).

comparisons with other studies of asteroid thermal inertia. Consistent with the small or medium thermal inertia value, the surface roughness is very high in our study, as the two quantities are usually anticorrelated. However, thermal skin depth calculated according to the formula from J. R. Spencer et al. (1989) is only 5 mm for Justitia, implying small regolith grain sizes.

Finally, since the main trigger of this work was an upcoming stellar occultation campaign, we generated the on-sky views of our newly created models. Figure 3 presents both solutions of Justitia's shape as on-sky views phased for the anticipated occultation moment on 2023 August 31 at 10:56 UT.

Our results have much wider applications: the reliable size and albedo constraints with the knowledge of thermal inertia and surface roughness of asteroid Justitia is going to facilitate the MBR Explorer mission planning, in situ operations, and landing. Also, the wealth of data obtained during the mission compared to premission results are going to provide a ground truth for asteroid studies based on remote sensing.

5. Discussion and Conclusions

Motivated by the planned space mission and upcoming favorable occultation event, we successfully attempted spin and shape reconstruction of the unusual D-type main-belt Justitia from lightcurves. Additionally, we also studied this body in the thermal aspect, which allowed us to obtain a good size estimate of 58 ± 2 km, pinpointing it to a much narrower range than the sizes available from previous studies (46.56–64.92 km). Previous size determinations of Justitia were based on the Simple Thermal Model (STM) (E. F. Tedesco et al. 2002), IRAS-STM model; (E. L. Ryan & C. E. Woodward 2010), and NEATM (e.g., J. R. Masiero et al. 2012), which use spherical shape approximation and other simplifying assumptions concerning the asteroid spin and thermophysical parameters to fit sparse thermal measurements. Here we provide detailed spin and shape solutions applied in a more sophisticated thermophysical model, free from such assumptions. As such, our model is the first full spin, shape, and size solution for asteroid Justitia, consistent with all the data used for its construction: a rich set of dense lightcurves, calibrated brightness measurements, and thermal infrared data. Connected to size, previously published

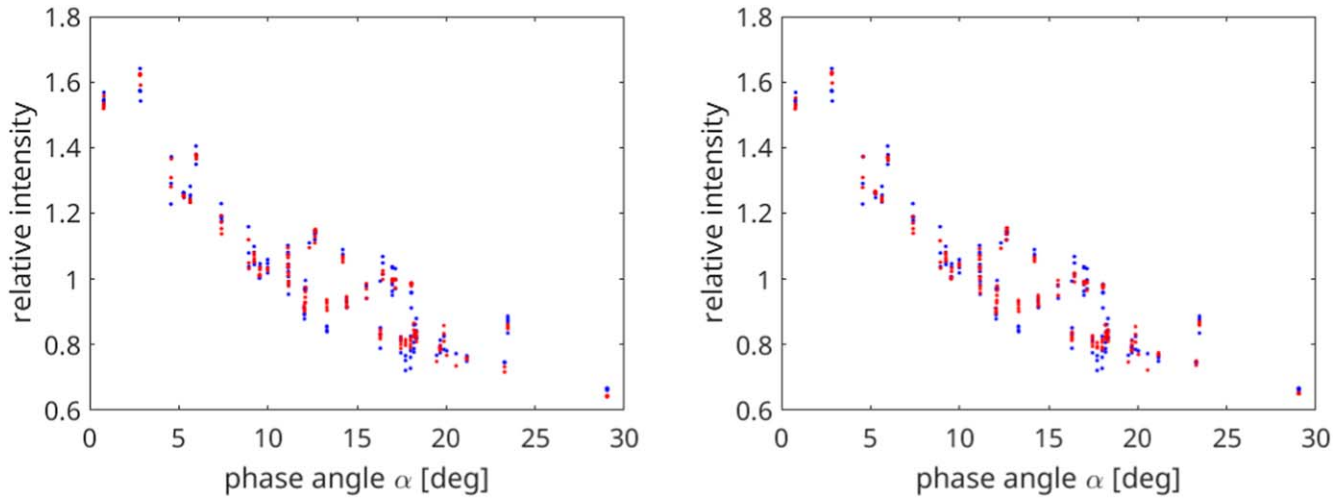


Figure 2. The model fit to normalized phase curve of (269) Justitia resulting from the CITPM: solution for pole 1 (left) and pole 2 (right). Calibrated brightness measurements have to be normalized in the modeling process in order not to overweight other types of data.

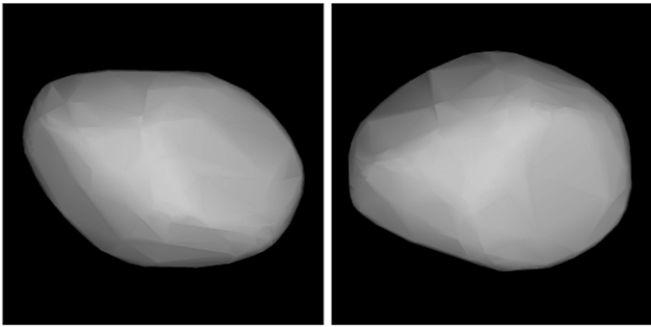


Figure 3. On-sky views of Justitia shape models from the CITPM phased for the 2023 August 31 occultation moment at 10:56 UT. North is up and east is left. Left plot: shape model for pole 1; right plot: same for pole 2 (see Table 1).

albedo values for Justitia were in a rather wide range from 0.061 (J. R. Masiero et al. 2012) to 0.130 (E. L. Ryan & C. E. Woodward 2010). Our value for albedo turns out to be even smaller (0.058 ± 0.006), consistent with the hypothesized origin of Justitia in the trans-Neptunian region of icy bodies, with a surface covered with darker organic material, later darkened even more by the organic ice reddening processes. Relatively small to medium thermal inertia supports a long history of the surface being influenced by micrometeorite bombardment, resulting in a layer of fine regolith on the surface. The thermal solution also suggests a high surface roughness, with a thermal skin depth of 5 mm.

As opposed to a previous sparse-data model published by J. Āurech et al. (2020), our high-resolution shape model of Justitia has a more realistic, smooth appearance, free from sharp edges and large planar sections, characteristic of models based on sparse-in-time data. Such data apparently do not contain full information on the whole shape. Still, models constructed on them are good at correctly reproducing spin axis position and sidereal period (J. Hanuř et al. 2016). The spin solution found by J. Āurech et al. (2020) is $\lambda_{p1} = 71^\circ$, $\beta_{p1} = -79^\circ$, and $\lambda_{p2} = 251^\circ$, $\beta_{p2} = -69^\circ$, with $P_{\text{sid}} = 33.129$ hr, placing the spin axis a few degrees from our solution and having consistent, though less precise, sidereal period of rotation (see Table 1). Also, our study resulted in a shape model with well-determined stretch along the rotation

axis, which has been a persisting weakness of shape models reconstructed from relative lightcurves only, as was the case in an initial version of our model.

Our model of the Justitia asteroid already proved useful for the occultation campaign planning and will be important for the MBR Explorer mission operations and science results. The initial results from the occultation campaign confirm our findings. They also clearly reject one of the mirror shape solutions, while confirming the other, thus breaking the spin ambiguity. For a detailed description of the occultation campaign and results see the accompanying paper by M. W. Buie et al. (2025).

Acknowledgments

We are grateful to Vadim Nikitin for contacting us with the occultation team, which motivated us to model asteroid Justitia just in time to support the occultation campaign planning. We thank Josef Āurech for enabling us to phase the new model of Justitia through the DAMIT service.

This work was supported by the National Science Centre, Poland, through grant No. 2020/39/O/ST9/00713. R.S. has received funding from the K-138962 grant of the National Research, Development and Innovation Office (NKFIH, Hungary). This paper was partially based on observations obtained at Sobaeksan Optical Astronomy Observatory (SOAO), which is operated by the Korea Astronomy and Space Science Institute (KASI). E.P. acknowledges the Europlanet 2024 RI project funded by the European Union's Horizon 2020 Research and Innovation Programme (grant agreement No. 871149).

Appendix

Additional Figures and Tables

Plots of the reduced infrared χ^2 versus thermal inertia (Figure 4), composite lightcurves in the visible from three apparitions (Figures 5 and 6), example fit of Justitia model to visible lightcurves (Figure 7), and infrared model fluxes compared to measured fluxes (Figure 8). Details of the observing campaign are given in Table 2.

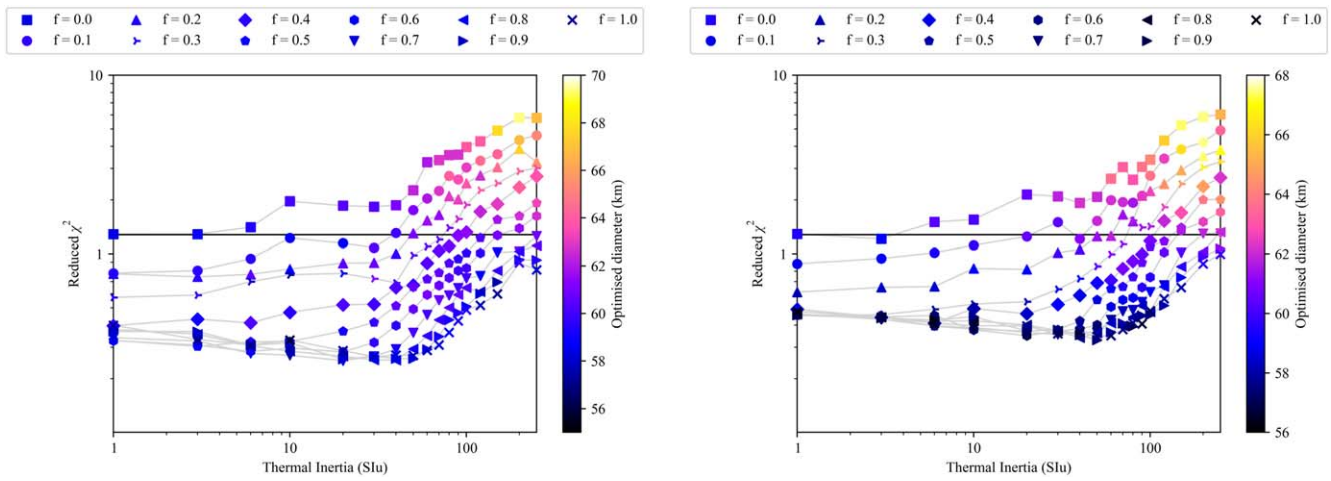


Figure 4. Reduced infrared χ^2 values vs. thermal inertia for various combinations of surface roughness (symbol coded) and optimized diameters of the equivalent surface sphere (color coded). Solutions for pole 1 (left) and for pole 2 (right). Due to the multitude of parameters, for surface roughness only the surface element coverage is shown (f), while the opening angle of spherical-section craters ranged from 10° to 90° . Higher opening angles provided better fit to thermal data.

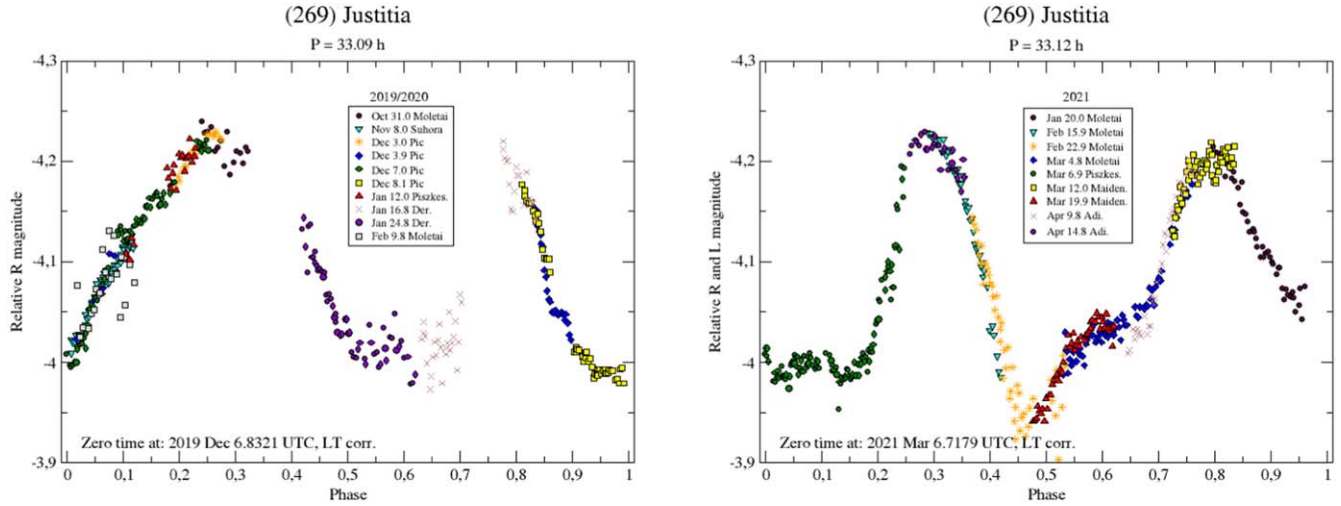


Figure 5. Composite lightcurves of (269) Justitia from the verge of the years 2019 and 2020 (left) and from the year 2021 (right).

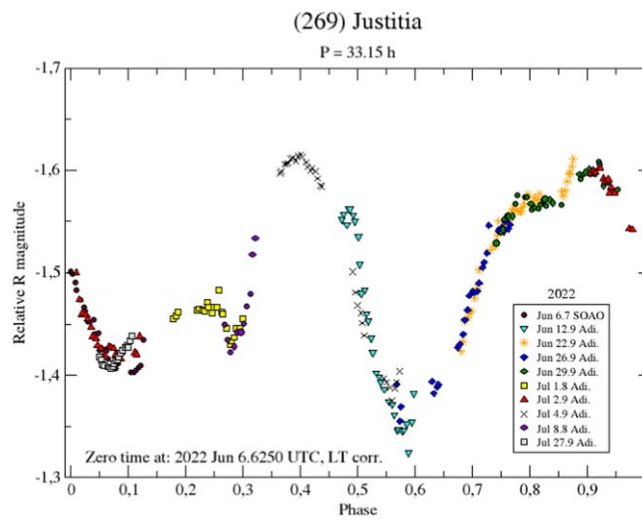


Figure 6. Composite lightcurve of (269) Justitia from the year 2022.

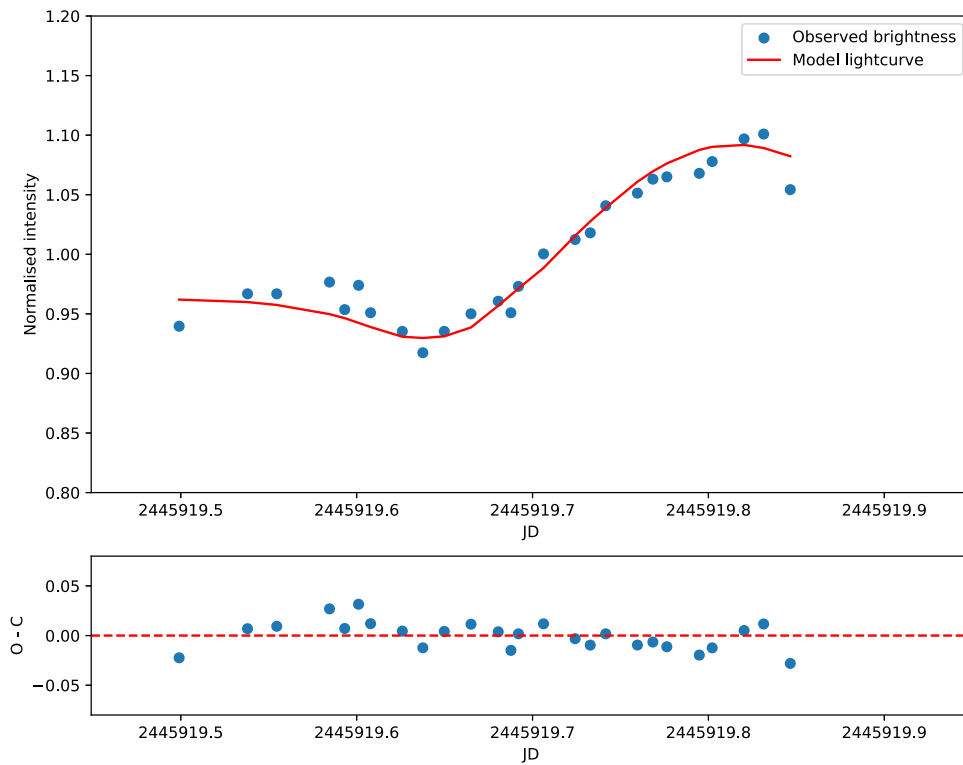


Figure 7. Example fit of Justitia model to visible lightcurves. Due to a slow rotation (33 hr period), each lightcurve covers only a small portion of the full period. (The data used to create this figure are available in the [online article](#).) (The complete figure set (51 images) is available in the [online article](#).)

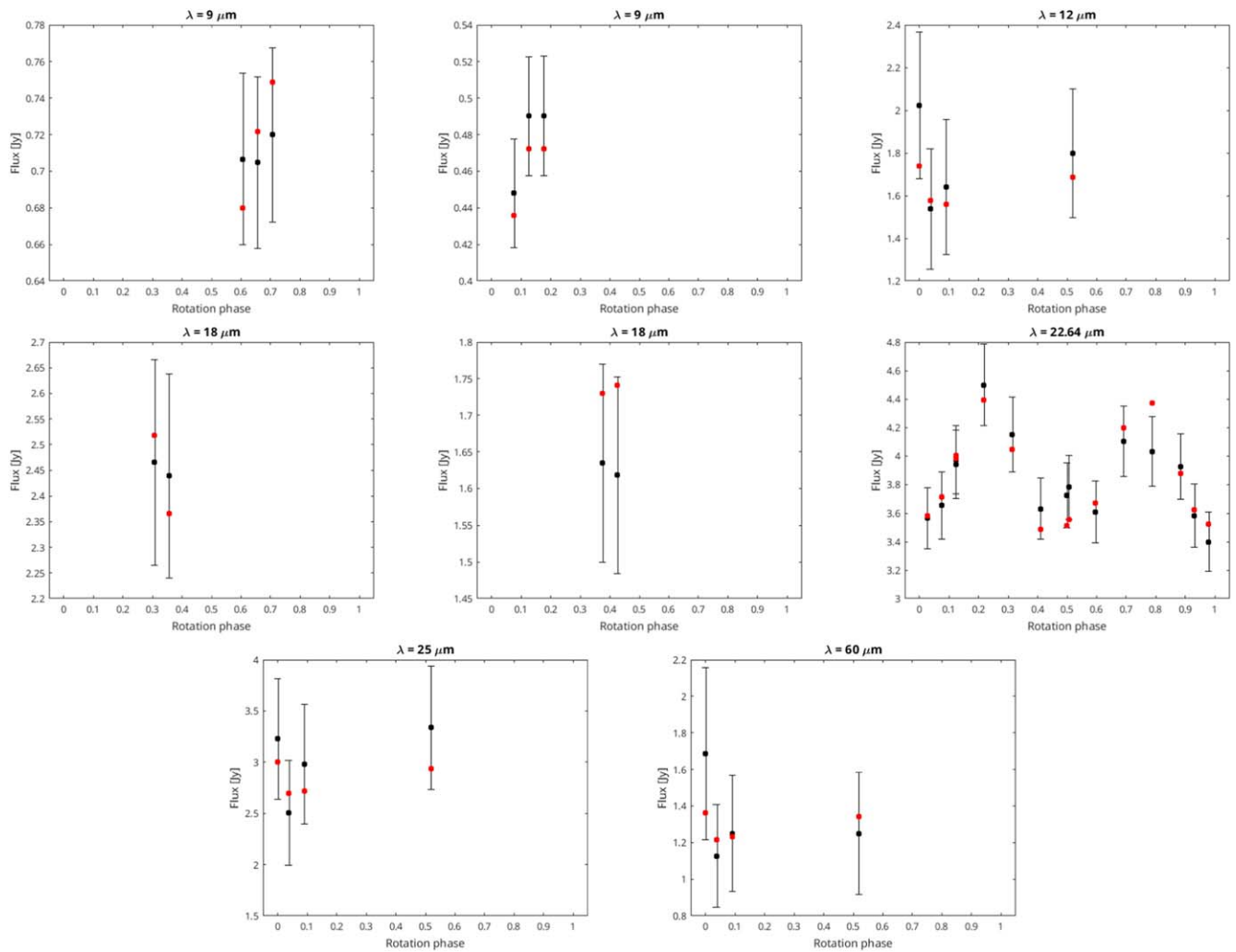


Figure 8. Asteroid Justitia infrared model fluxes (red circles) compared to measured fluxes in various bands indicated in each plot (black circles). Infrared measurements spaced by more than 100 days are shown in separate plots.

Table 2
Details of the Photometric Campaign for (269) Justitia

Date	N_{lc}	λ (deg)	Phase Angle (deg)	Observer	Site
1984 Aug 6.2–1984 Aug 15.2	5	296–297	8–13	M. A. Barucci et al. (1992)	ESO, La Silla, Chile
2006 Dec 11.9–2006 Dec 13.9	2	43	12	P. Antonini, R. Behrend	Observatoire des Hauts Patys, France
2015 Nov 21.4–2016 Jan 3.2	11	85–94	2–11	F. Pilcher (2016)	Organ Mesa Observatory, NM, USA
2017 Feb 26.7–2017 Mar 2.7	5	162–163	0–2	T.-S. Yeh et al. (2020)	Purple Mountain Observatory, PR China
2019 Oct 31.0–2020 Feb 9.8	2	66–79	13–18	E. Pakštienė	Molėtai, Lithuania
2019 Nov 8.0	1	78	10	M. Drózdź	Mount Suhora, Poland
2019 Dec 3.0–2019 Dec 8.1	4	72–73	3	S. Fauvaud, M. Fauvaud	Pic du Midi Observatory, France
2020 Jan 12.0	1	66	13	G. Csörnyei	Piszkéstető, Hungary
2020 Jan 16.8–2020 Jan 24.8	2	65–65	14–16	V. Kudak, V. Perig	Derevinka, Ukraine
2021 Jan 20.0–2021 Mar 4.8	4	137–147	2–9	E. Pakštienė	Molėtai, Lithuania
2021 Mar 6.9	1	137	10	R. Szakáts	Piszkéstető, Hungary
2021 Mar 12.0–2021 Mar 19.9	2	135–136	12–14	A. Jones	Maidenhead, UK
2021 Apr 9.8–2021 Apr 14.8	2	134–135	19–20	W. Ogłóza	Adiyaman, Turkey
2022 Jun 6.7	1	287	15	D.-H. Kim, M.-J. Kim	SOAO, South Korea
2022 Jun 12.9–2022 Jul 27.9	9	278–286	4–13	W. Ogłóza	Adiyaman, Turkey

Note. Table shows observing dates, number of lightcurves, range of ecliptic longitudes of the target, Sun–target–observer phase angles, the observer’s name (or paper citation in cases of published data), and the observing site. SOAO stands for Sobaeksan Optical Astronomy Observatory.

References

- Barucci, M. A., di Martino, M., & Fulchignoni, M. 1992, *AJ*, **103**, 1679
- Buie, M. W., AlMazmi, H., Hayne, P., et al. 2025, Occultation based Size and Shape of (269) Justitia, *PSJ*, **6**, 61
- Delbo', M., Mueller, M., Emery, J. P., Rozitis, B., & Capria, M. T. 2015, in Asteroid Thermophysical Modeling, ed. W. F. Botte, F. E. DeMeo, & P. Michel (Tucson, AZ: Univ. Arizona Press), 107
- DeMeo, F. E., Binzel, R. P., Slivan, S. M., & Bus, S. J. 2009, *Icar*, **202**, 160
- Đurech, J., Delbo', M., Carry, B., Hanuš, J., & Alí-Lagoa, V. 2017, *A&A*, **604**, A27
- Đurech, J., Tonry, J., Erasmus, N., et al. 2020, *A&A*, **643**, A59
- El-Maarry, M. R., Landis, M. E., Capaccioni, F., & Filacchione, G. 2023, in LPI Contribution, 2851 (Houston, TX: Lunar and Planetary Inst.), 2385
- Filacchione, G., Ciarniello, M., De Sanctis, M. C., et al. 2023, in LPI Contribution, 2851 (Houston, TX: Lunar and Planetary Inst.), 2157
- Gil-Hutton, R., & Garcia-Migani, E. 2017, *A&A*, **607**, A103
- Hanuš, J., Đurech, J., Oszkiewicz, D. A., et al. 2016, *A&A*, **586**, A108
- Hapke, B. 1981, *JGR*, **86**, 3039
- Hapke, B. 1984, *Icar*, **59**, 41
- Hapke, B. 1986, *Icar*, **67**, 264
- Hasegawa, S., Marsset, M., DeMeo, F. E., et al. 2021, *ApJL*, **916**, L6
- Kaasalainen, M., & Torppa, J. 2001, *Icar*, **153**, 24
- Kaasalainen, M., Torppa, J., & Muinonen, K. 2001, *Icar*, **153**, 37
- Keihm, S. J. 1984, *Icar*, **60**, 568
- Lagerros, J. S. V. 1996, *A&A*, **310**, 1011
- Lagerros, J. S. V. 1997, *A&A*, **325**, 1226
- Lagerros, J. S. V. 1998, *A&A*, **332**, 1123
- Lim, L. F., McConnochie, T. H., Bell, J. F., & Hayward, T. L. 2005, *Icar*, **173**, 385
- Mahlke, M., Carry, B., & Mattei, P. A. 2022, *A&A*, **665**, A26
- Marciniak, A., Đurech, J., Alí-Lagoa, V., et al. 2021, *A&A*, **654**, A87
- Marciniak, A., Ďurech, J., Choukroun, A., et al. 2023, *A&A*, **679**, A60
- Marciniak, A., Pilcher, F., Oszkiewicz, D., et al. 2015, *P&SS*, **118**, 256
- Masiero, J. R., Mainzer, A. K., Bauer, J. M., et al. 2020, *PSJ*, **1**, 5
- Masiero, J. R., Mainzer, A. K., Grav, T., et al. 2012, *ApJL*, **759**, L8
- Morbidelli, A., Levison, H. F., Tsiganis, K., & Gomes, R. 2005, *Natur*, **435**, 462
- Mueller, M., Marchis, F., Emery, J. P., et al. 2010, *Icar*, **205**, 505
- Neugebauer, G., Habing, H. J., van Duinen, R., et al. 1984, *ApJL*, **278**, L1
- Pál, A., Szakáts, R., Kiss, C., et al. 2020, *ApJS*, **247**, 26
- Pilcher, F. 2016, *MPBu*, **43**, 135
- Raponi, A., Filacchione, G., Ciarniello, M., et al. 2023, in LPI Contribution, 2851 (Houston, TX: Lunar and Planetary Inst.), 2450
- Reed, H., Al Ameri, M. O., Landis, M. E., et al. 2023, in LPI Contribution, 2851 (Houston, TX: Lunar and Planetary Inst.), 2366
- Rozitis, B., Green, S. F., MacLennan, E., & Emery, J. P. 2018, *MNRAS*, **477**, 1782
- Ryan, E. L., & Woodward, C. E. 2010, *AJ*, **140**, 933
- Sagan, C., & Khare, B. N. 1979, *Natur*, **277**, 102
- Spencer, J. R., Lebofsky, L. A., & Sykes, M. V. 1989, *Icar*, **78**, 337
- Szakáts, R., Müller, T., Alí-Lagoa, V., et al. 2020, *A&A*, **635**, A54
- Tedesco, E. F., Noah, P. V., Noah, M., & Price, S. D. 2002, *AJ*, **123**, 1056
- Tonry, J. L., Denneau, L., Heinze, A. N., et al. 2018, *PASP*, **130**, 064505
- Tsiganis, K., Gomes, R., Morbidelli, A., & Levison, H. F. 2005, *Natur*, **435**, 459
- Usui, F., Kuroda, D., Müller, T. G., et al. 2011, *PASJ*, **63**, 1117
- Vernazza, P., & Beck, P. 2017, in Planetesimals: Early Differentiation and Consequences for Planets, ed. L. T. Elkins-Tanton & B. P. Weiss (Cambridge: Cambridge Univ. Press), 269
- Vernazza, P., Beck, P., Ruesch, O., et al. 2022, *ExA*, **54**, 1051
- Vokrouhlický, D., Bottke, W. F., & Nesvorný, D. 2016, *AJ*, **152**, 39
- Wright, E. L., Eisenhardt, P. R. M., Mainzer, A. K., et al. 2010, *AJ*, **140**, 1868
- Yeh, T.-S., Li, B., Chang, C.-K., et al. 2020, *AJ*, **160**, 73